Comparing Internal and External Cathode Boundary Position in a Hall Thruster Particle Simulation

IEPC-2017-402

Presented at the 35th International Electric Propulsion Conference
Georgia Institute of Technology • Atlanta, Georgia • USA
October 8 – 12, 2017

Shinatora Cho[1]
Japan Aerospace Exploration Agency, Sagamihara, Kanagawa, 252-5210, Japan

Kenichi Kubota[2]
Japan Aerospace Exploration Agency, Chofu, Tokyo, 182-8522, Japan

Hiroki Watanabe[3]
Tokyo Metropolitan University, Hino, Tokyo, 191-0065, Japan

Kentaro Hara[4]
Texas A&M University, College Station, Texas, 77843, USA

and

Ikkoh Funaki[5]
Japan Aerospace Exploration Agency, Sagamihara, Kanagawa, 252-5210, Japan

Abstract: Coupling between the cathode and thruster is an intensively investigated research topic of Hall thrusters, known to have influence on beam divergence and potential structure. The effects of cathode positions are numerically studied by parameterizing the location of cathode boundary in the computation domain of a 2D fully kinetic particle-in-cell simulation. Simulation results have shown that placing the cathode near the center of symmetry, representing an internally mounted configuration, exhibits higher beam efficiency than that of an external case by 2%, which is consistent with previous measurements. Detailed comparison of plasma parameters suggests that the change in beam optics is caused by the difference of potential structure inside the channel due to the cathode coupling dynamics.

Nomenclature

E	=	electric field
e	=	unit charge
I_{beam}	=	ion beam current
I_{inj}	=	electron injection current
I_z	=	axial ion beam current
j	=	current density
k	=	Boltzmann constant

[1] Researcher, Research and Development Directorate, choh.shinatora@jaxa.jp..
[2] Researcher, Aeronautical Technology Directorate, kkubota@chofu.jaxa.jp.
[3] Research Associate, Department of Aerospace Engineering, hwatanabe@tmu.ac.jp.
[4] Assistant Professor, Department of Aerospace Engineering, Texas A&M University, khara@tamu.edu
[5] Associate Professor, Institute of Space and Astronautical Science, funaki@isas.jaxa.jp.

L_c = channel length
h = channel height
m = electron mass
n = electron number density
R_c = channel center
r = radial position
S = area
T_e = electron temperature
v_e = electron speed
z = axial position
μ = electron mobility
ν = electron collision frequency
ρ = charge density
Ψ_B = beam efficiency
Ω_e = electron Hall parameter

I.Introduction

CATHODE is an essential component for Hall thruster operation which neutralizes the ion beam and supplies electrons to the thruster anode. The cathode-to-thruster plasma coupling is considered to have substantial influence on the thruster discharge mainly by means of beam divergence and potential structure.[1] The position of cathode mount is a method of controlling the cathode coupling which have been investigated by different institutes,[2-4] and the "internally mounted" configuration was reported to be effective in confinement of beam divergence and improvement of beam symmetry.[5] In this configuration, the cathode is mounted at the center of the thruster so it is suggested that the enhanced plasma density in-between the discharge ring led to the improved potential structure and thus the efficiency.[5] The related plasma properties and structure were measured by various probes, and also numerically reproduced by fluid simulation using empirical diffusion parameters, which suggests the cathode plume and its interactions with the ion beam is important for understanding the discharge of Hall thrusters.[6] JAXA is developing a 6-kW Hall thruster system for an all-electric propulsion satellite, which has the capability of mounting the cathode in the thruster center.[7] Experimental and numerical characterization and evaluation of the cathode position is ongoing,[8] and in this study, we use fully-kinetic particle simulation to model the discharge of a representative Hall thruster with cathode boundary to investigate the mechanism of merits in internal cathode mount configurations. The simulation code used in this study is an axial-radial two-dimensional fully kinetic Particle-In-Cell code developed in JAXA called JHAST f/p. Following our previous studies,[9,10] no artificial transport models are included. Three simulation cases were run for different cathode boundary positions, and the ion current profile, electric field structure, and electron number density as well as cross-field transport distributions are compared and discussed.

II.Numerical Methods

JHAST f/p, an axial-radial two-dimensional fully kinetic Particle-In-Cell code is used in this study. This code simulates particles including neutrals, electrons, and ions up to triple charge and all kinds of simulated particles are tracked directly solving the equation of motion. Electric field is calculated by solving Poisson equation, and linear weighting between the field and the charged particles is adopted. Inter-particle collisions are implemented in a Monte-Carlo-Collision (MCC) manner. Table 1 summarizes the detail of the numerical settings. No artificial permittivity technique is used in this study; however, the artificial electron mass model is implemented to speed-up the computation. The detail of the employed physics recovering model and its verification and validation can be found in the previous studies.[9] Because our recent study suggested the code can at least qualitatively capture the electron turbulence transport across the magnetic field without implementing any artificial anomalous diffusion models,[10] no additional transport models are used in this study either.

Table 1. Numerical settings.

Item	value
Timestep	1.0×10^{-10} s
Grid spacing	2.0×10^{-4} m
Artificial mass ratio	Electron mass multiplied by $f^2 = 625$
	Magnetic field correction $f_B = f^{1/2} = 5$
Macro particle weight	1.0×10^7
Particle species	e^-, X_e^+, X_e^{2+}, X_e^{3+}
Collision	$e^- - X_e$ elastic scattering
	$e^- - X_e$ excitation
	$e^- - X_e$ ionization
	$e^- - X_e^+$ ionization
	$e^- - X_e^{2+}$ ionization
	$X_e - X_e^+$ CEX
	$X_e - X_e^{2+}$ CEX
	$X_e - X_e^{3+}$ CEX
	Coulomb collisions
Xenon momentum accommodation coefficient	0.926
Xenon energy accommodation coefficient	0.8

A. Thruster and Computational Domain

A representative geometry of an SPT-100 like Hall thruster is simulated in this study. The thruster geometry and operation conditions tabulated in table 2 are set to be the same as the previous literatures.[11] A modeled magnetic field design is used because the detailed design information of the original thruster is unavailable. The magnetic flux density is designed to take its maximum at the discharge channel exit.

Table 2. Thruster geometry and operation conditions.

	Item	Value
Thruster geometry	Outer channel diameter	100 mm
	Channel width	15.6 mm
	Channel length	25 mm
Thruster operation condition	Discharge voltage	300 V
	Beam to keeper voltage	10 V
	Anode mass flow rate	5 mg/s
	Max magnetic flux density at channel center	16 mT
	Anode temperature	800 K
	Wall temperature	800 K

B. Boundary conditions

The computational domain and setting of the boundary conditions are summarized in figure 1. Uniform rectangular grid is used in *r-z* cylindrical coordinate. The area near the axis of symmetry is excluded from the domain because of the computational cost. Due to the small cell volume near the axis of symmetry, it is considered particle split and merge technique is necessary or otherwise approximately two orders of magnitude greater simulation particle number will be required. The extension of computational domain to the axis and the implementation of split/merge technique are reserved to be our future work.

Dirichlet condition was used for the field at the anode and cathode. Since the beam to keeper voltage is assumed to be 10 V as shown in table 2, the anode potential was fixed to 290 V (=Discharge voltage – Beam to keeper voltage). Xe propellant of 5 mg/s mass flow rate is injected from a 2-mm slit located at the channel center. Neutrals and ions impinging the anode surface are diffused according to the momentum and thermal accommodation factors assumed in table 1. Charges are accumulated on the Boron Nitride (BN) walls and the particle deflection on the wall surface is treated the same manner as the anode. Neumann condition is applied at the plume free-space boundaries that the electric field is fixed to zero. All of the particles crossing the plume boundary are lost. Quasi-neutrality electron

injection scheme is used at the plume boundaries to avoid any artificial effects caused by the boundary-induced charge imbalance.[11] The local electron injection current I_{inj} is determined as follows:

$$I_{inj} = e\rho v_e S \tag{1}$$

where, e is unit charge, ρ is the local charge density, v_e is electron speed, and S is the area of the boundary. Note I_{inj} is set to zero if ρ is negative. The initial energy of injected electrons is assumed to be 2 eV.

Three different cases of cathode boundary placement are simulated: INT, EXT, and NONE. The INT case representing the internal cathode configuration, having the cathode line at the inner plume boundary 10 mm downstream from the channel exit with 3 mm long. Potential is fixed to 0 V and cathode flow of 0.35 mg/s is injected assuming the cathode flow fraction to be 0.07. The total electron injection current is determined by the discharge current I_d, and is uniformly distributed to the cathode line. Likewise, the cathode line is placed at the outer plume boundary in EXT case representing the external cathode configuration. Note that the cathode line is a ring in the simulation so that the three-dimensional effects in experiment are omitted and unable to be captured in this study. However, still it is considered to be useful to discuss about the qualitative difference cause by the placement of cathode boundary. The last case NONE represents the configuration of idealistic ion beam neutralization, having the cathode line at the entire right plume boundary. No Xe or electrons are actively injected in this case, so all of the electrons necessary for the discharge are provided passively from the plume and cathode line with fixed potential according to Eq. 1.

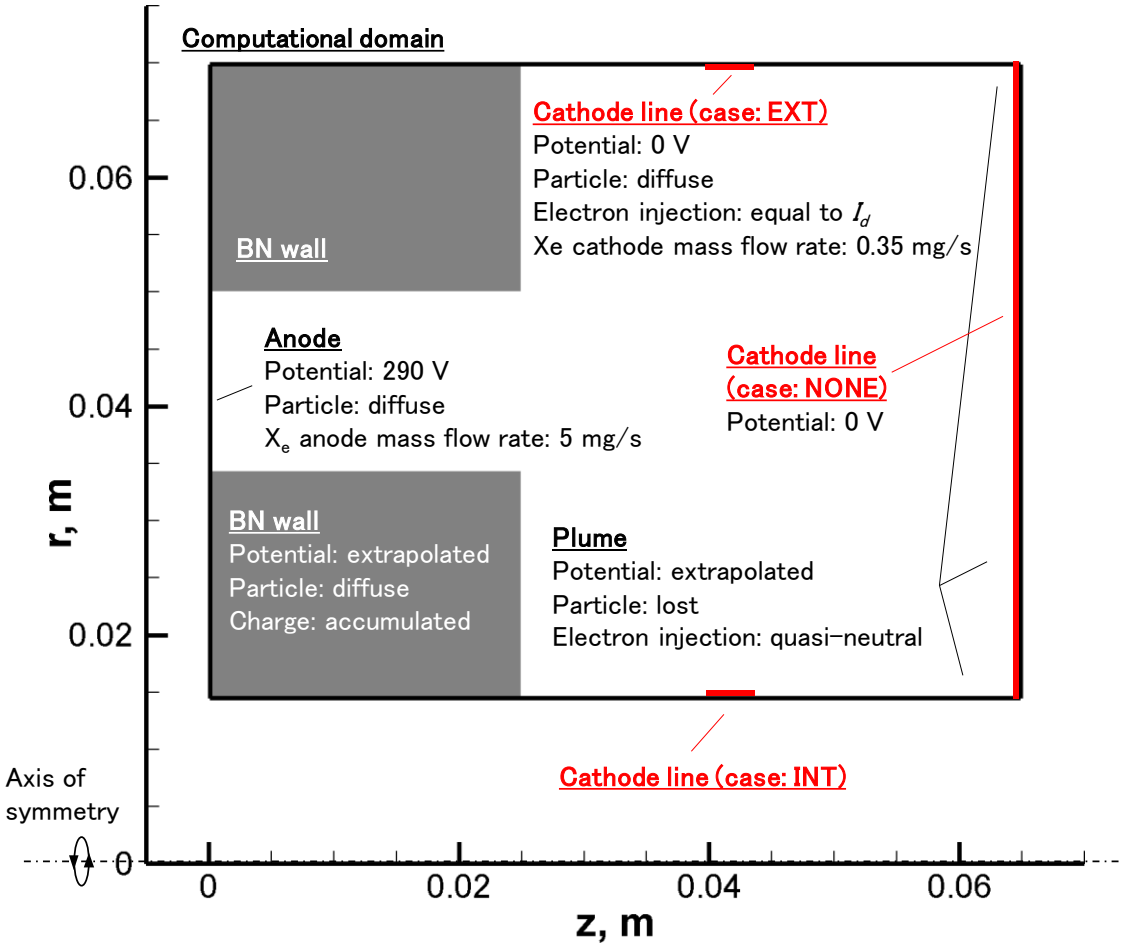

Figure 1. Computational domain and setting of boundary conditions. *Three simulation cases were conducted for different cathode boundary placements: INT, EXT, and NONE. The potential of the right plume boundary was fixed to 0 V in the NONE case, whereas it was extrapolated with no gradient in other two cases.*

III.Results and Discussion

It is reported in previous experimental studies that one of the most important findings of the internal cathode configuration is it can improve the beam divergence.[5] This trend was successfully captured in the three simulation cases that the beam efficiency defined as follows:

$$\Psi_B = \left(\frac{I_z}{I_{beam}}\right)^2 \tag{2}$$

were respectively 0.91, 0.89, and 0.91 for NONE, EXT, and INT case. Here, I_z is the axial component of ion current and I_{beam} is the ion beam current. Therefore, it is suggested that the inward cathode placement can achieve higher beam efficiency than the outward case, which is almost equal to the idealistic beam neutralization situation. Although this result is consistent qualitatively with experimental observation, it should be noted that the three-dimensional effect of the external cathode configuration is not included in this simulation, so quantitatively the difference between the two configurations can be underestimated in this simulation. In order to investigate what caused this difference in the simulation, plasma properties are detailed in following sections.

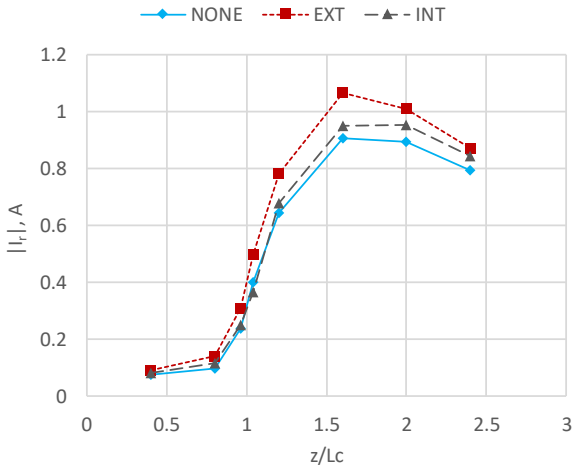

(a) Radial ion current

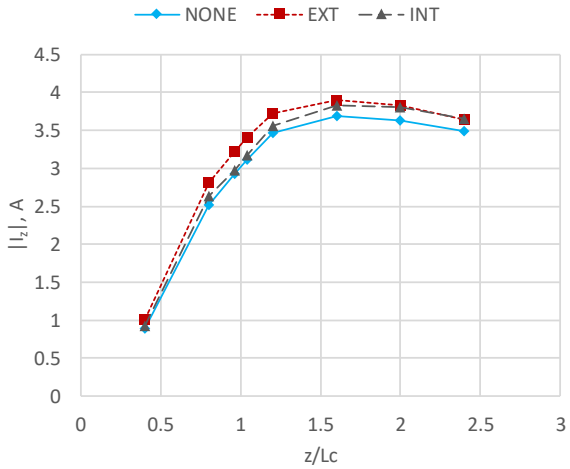

(b) Axial component of ion current

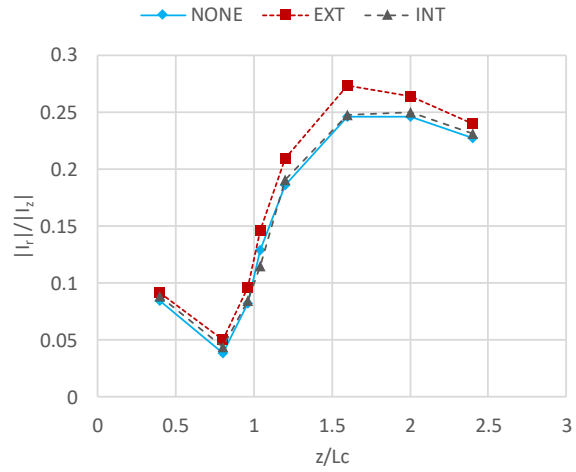

(c) Ratio of radial and axial ion currents

Figure 2. Simulation result of ion current profile along the thruster axis. *Ion current is integrated in the radial direction at each z position. Thruster anode is located at $z/L_c=0$ and the channel exit is at $z/L_c=1$.*

A. Ion current

Simulated ion current profiles are shown in Fig. 2(a) and (b). The horizontal axis is normalized by the channel length L_c. The overall trend is the ion current increases from the upstream channel up to z/L_c, and slightly decreases until the end of computational domain. The decrease of the ion current outside the channel is simply because the ion beam in large angle is lost from the inner and outer plume boundaries. It can be seen that like general understanding of Hall thrusters, most of the ion current is generated inside the channel, and it start to expand in radial direction outside the channel. The EXT case exhibited highest ion current both in radial and axial direction, whereas the NONE case was the lowest. The ratio of radial and axial ion current indicating the beam divergence is presented by Fig. 2(c). As expected, the result is consistent with the beam efficiency that the ratio or the beam divergence was the highest in the EXT case. It is interesting though that the difference of the ratio starts from the area near the channel exit, suggesting the placement of cathode can influence the plasma structure very close to or even inside the channel.

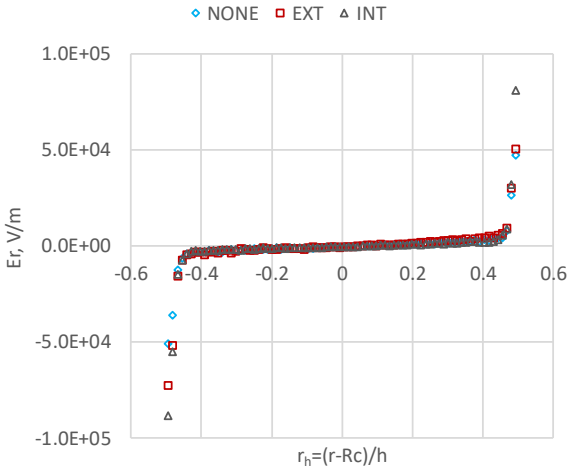

(a) Radial electric field E_r at z/Lc=0.96

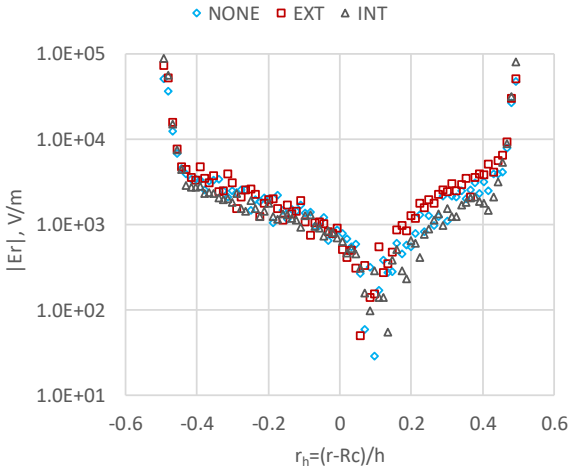

(b) $|E_r|$ at z/Lc=0.96 in log scale

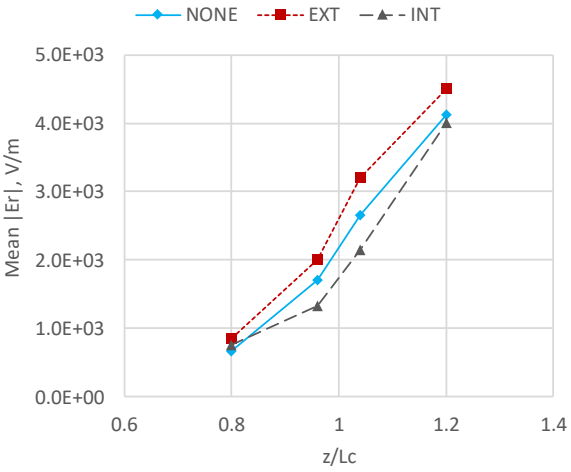

(c) $|E_r|$ averaged within $|r_h| < 0.45$

Figure 3. Simulation result of radial electric field. *Radial position is normalized by channel height, where 0 is the channel center, -0.5 is the inner wall, and 0.5 is the outer wall.*

B. Radial electric field

Radial electric field E_r, which is considered to be the direct cause of the beam divergence, is presented in Fig. 3. To specify the exact structure of radial ion acceleration, the $|E_r|$ profile in radial direction at the z position of $z/L_c = 0.96$ is extracted in Fig. 3(a) and (b). The plot of E_r in log scale is shown in Fig. 3(a), where it is visible that very strong electric field exists near the walls representing the dielectric wall sheath. The thickness of the sheath observed is approximately 0.6 mm, which is several times the Debye length and is considered to be reasonable. It can be seen

that the bulk plasma region responsible for the beam divergence is roughly the area of $|r_h| < 0.45$, where r_h is the radial position r normalized by the channel height h relative to the channel center R_c as:

$$r_h = \frac{r - R_c}{h} \tag{3}$$

Note $|r_h| = 0.5$ denotes the inner and outer wall. The electric field in bulk plasma region can be specified in Fig. 3(b), which presents the radial plot of $|E_r|$ in log scale. It is notable that the minimum of $|E_r|$ equals to the potential peak is located at the slightly outside than the channel center, which indicates the equipotential line is slanted toward the inner wall probably because of the magnetic field topology. Interestingly, nontrivial difference of $|E_r|$ between the three simulation cases can be found mainly at the region between the potential peak and the outer wall but not the inner wall. Thus, it is suggested that the difference of cathode position, especially the external configuration, changed mainly the outer half of the potential structure.

The axial profile of averaged $|E_r|$ is shown in Fig. 3(c). The average is taken in radial direction within the bulk plasma area $|r_h| < 0.45$. As expected, the result shown in Fig. 3(c) suggests the $|E_r|$ which causes the ion radial acceleration and thus accounts for the beam divergence, is the highest in the EXT case. Furthermore, the difference of $|E_r|$ starts from the near exit area, which is consistent with the ion current profile.

C. Electron number density and mobility

To seek for the reason of the electric field difference, axial profile of electron number density is shown in Fig. 4. and 5. The density profile on the channel center line shown by figure 4, where the horizontal axis is again the axial position relative to the channel length. The result suggests the density is highest at upstream of the channel exit for all cases. The second density peak can be found near the anode is considered to be caused by the high-density propellant injection through the 2-mm slit. In comparison among the three cases, NONE and INT have relatively the same profile, whereas the density peak in EXT seems to be pushed inside toward the anode. The plasma density at outward of the channel is shown in Fig. 5. The vertical axis denotes the ratio of plasma density on the $r_h = 0.25$ line relative to that of the channel center line. The difference between the three simulation cases can be found around the region slightly outside the channel exit, showing the ratio of plasma density is higher in the EXT case. This result means the plasma density at the outer half of the beam is relatively high in the EXT case than the others, which is probably due to the cathode boundary is placed outward. Higher plasma density leads to higher electron mobility, which is considered to results in the plasma structure pushed upstream at the outer half of the channel leading to the increase of radial electric field and beam divergence eventually.

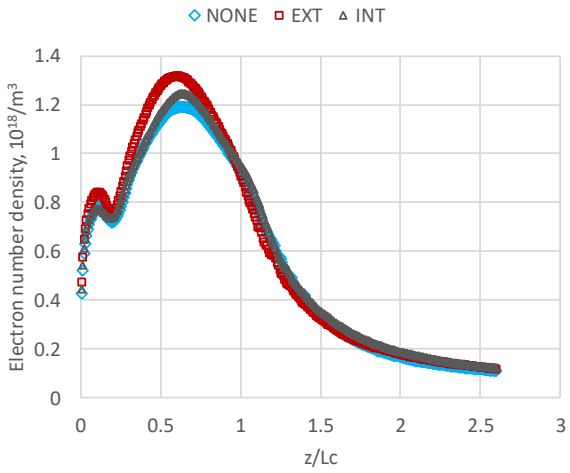

Figure 4. Simulation result of electron number density on the channel center line. *Thruster anode is located at z/L_c=0 and the channel exit is at z/L_c=1.*

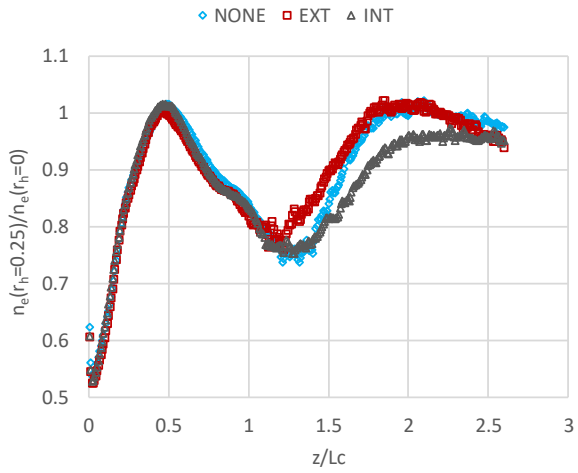

Figure 5. Electron number at r_h=0.25 relative to the channel center line. *The ratio is calculated at each z position.*

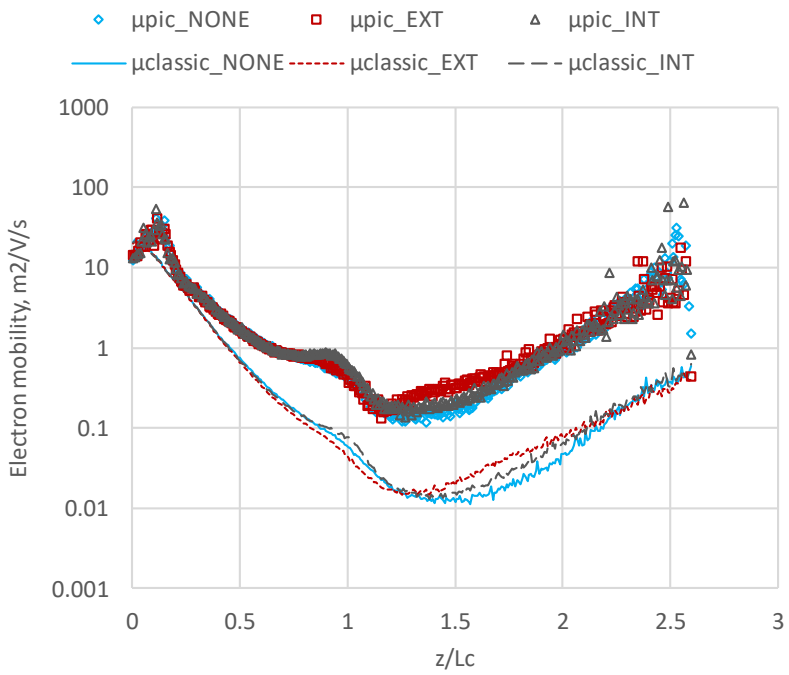

Figure 6. Simulation result of electron mobility at r_h=0.25. *Lines show the electron mobility calculated according to the classical diffusion theory, whereas the symbols are the effective mobility as Eq. 5.*

Electron mobility on the $r_h = 0.25$ line is presented in Fig. 6. The lines show the electron mobility calculated according to the classical diffusion theory as:

$$\mu_{classic} = \frac{1}{1+\Omega_e{}^2}\frac{e}{m\nu}. \tag{4}$$

where $\Omega_e = \omega_c/\nu$ is electron Hall parameter, $\omega_c = eB/m$ is the electron cyclotron frequency, and ν is the electron collision frequency sampled from each cell. On the other hand, the symbols denote the effective mobility based on the actual electron current in the simulation is computed according to Koo et al.,[12] as:

$$\mu_{pic} = \frac{j_{e\perp}}{E_z + \frac{kT_e}{e}\frac{1}{n}\frac{\partial n}{\partial z}}. \tag{5}$$

where $j_{e\perp}$ is the electron current density across the magnetic field, E_z is axial electric field, T_e is electron temperature, and n is plasma number density. It is clear even in log scale that the EXT case exhibits higher electron mobility than the other two cases at the near-exit plume region, which supports the discussion made above for the plasma density. Notably, the difference of electron mobility occurs both in classical and effective ones, and the ratio between them remains to be insensitive. It is thus reconfirmed that the effects of cathode boundary placement observed in this study are likely to be caused by the change of plasma density rather than the change of turbulent state. Because the azimuthal dynamics are neglected in this 2D axisymmetric framework, a full 3D simulation is required for looking at the turbulence effects for the external cathode-coupling regime. The detailed correlation between the electron turbulence transport and the cathode boundary position is reserved to be a future work.

IV.Conclusion

To investigate the influence of cathode position to a Hall discharge, axisymmetric particle kinetic simulation was conducted for different cathode boundary placements. The results have shown that the case representing the internally mounted configuration exhibits 2% higher beam efficiency than the case of external mount, which is qualitatively consistent with previous experimental observations. The comparison of plasma property distributions revealed that the difference in ion beam optics is caused by the potential structure not only near the cathode boundary but also near

the channel exit. The radial electric field increasing the beam divergence is considered to be resulted from the changes of plasma density and electron mobility.

Acknowledgments

The authors acknowledge that the computer simulation was performed on the KDK computer system at Research Institute for Sustainable Humanosphere, Kyoto University.

References

[1] K. K. Jameson, D. M. Goebel, R. R. Hofer and R. M. Watkins, "Cathode coupling in Hall thrusters," in Proceedings of the 30th International Electric Propulsion Conference, Florence, IEPC-2007-278, 2007.

[2] Jason D. Sommerville and Lyon B. King, "Effect of Cathode Position on Hall-Effect Thruster Performance and Cathode Coupling Voltage," 43rd AIAA/ASME/SAE/ASEE Joint Propulsion Conference & Exhibit 8 - 11 July 2007, Cincinnati, OH. AIAA 2007-5174.

[3] McDonald, M. S., Gallimore, A. D., "Cathode Position and Orientation Effects on Cathode Coupling in a 6-kW Hall Thruster," in Proceedings of the 34th International Electric Propulsion Conference, IEPC-2009-113, 2009.

[4] Xu, K. G., Walker, M. L. R., "Effect of External Cathode Azimuthal Position on Hall-Effect Thruster Plume and Diagnostics," Journal of Propulsion and Power, Vol. 30, No. 2 (2014), pp. 506-513.

[5] Hofer, R. et al. "Effects of Internally-Mounted Cathodes on Hall Thruster Plume Properties," IEEE Transactions on Plasma Science, Special Issue on Plasma Propulsion. (2008).

[6] Ortega, A. L., Mikellides, I. G., "The importance of the cathode plume and its interactions with the ion beam in numerical simulations of Hall thrusters," in Proceedings of the 34th International Electric Propulsion Conference, Hyogo-Kobe, IEPC-2015-310, 2015.

[7] Funaki, I., Iihara, S., Cho, S., Kubota, K., Watanabe, H., Fuchigami, K., Tashiro, Y., "Laboratory Testing of Hall Thrusters for All-electric Propulsion Satellite and Deep Space Explorers," 52nd AIAA/SAE/ASEE Joint Propulsion Conference, AIAA 2016-4942,2016, Salt Lake City.

[8] Kubota, K., Cho, S., Watanabe, H., Funaki, I., "Hybrid-PIC Simulation of Hall Thruster with Internally Mounted Cathode," in Proceedings of the 35th International Electric Propulsion Conference, Atlanta, GA, IEPC-2017-426.

[9] Cho, S., Komurasaki, K., Arakawa, Y., "Kinetic Particle Simulation of Discharge and Wall Erosion of a Hall Thruster," Pysics of Plasmas, 20, 063501 (2013), DOI: 10.1063/1.4810798.

[10] Cho, Shinatora, et al. "Study of electron transport in a Hall thruster by axial–radial fully kinetic particle simulation," Physics of Plasmas (1994-present) 22.10 (2015): 103523.

[11] Cho, S., Watanabe, H., Kubota, K., Funaki, I., "The Effects of Cathode Boundary Condition on Particle Simulation of a SPT-100-like Hall Thruster," 52nd AIAA/ASME/SAE/ASEE Joint Propulsion Conference & Exhibit, Salt Lake City, UT, AIAA Paper 2016-4728, 2016.

[12] Koo, J. W., and Boyd, I. D., "Modeling of anomalous electron mobility in Hall thrustersPhys. Plasmas, 13, 033501 (2006)," doi: 10.1063/1.2172191.